AAPS PharmSciTech (2022) 23: 104
https://doi.org/10.1208/s12249-022-02257-1

RESEARCH ARTICLE

Rethinking Breast Cancer Chemoprevention: Technological Advantages and Enhanced Performance of a Nanoethosomal-Based Hydrogel for Topical Administration of Fenretinide

Alexsandra Conceição Apolinário[1] · Giovanna Cassone Salata[1] · Marcelo Medina de Souza[2] · Marlus Chorilli[3] · Luciana Biagini Lopes[1]

Received: 3 February 2022 / Accepted: 22 March 2022 / Published online: 5 April 2022

Abstract

Herein, we developed an ethosomal hydrogel based on three types of ethosomes: simple, mixed (surfactant-based micelles and lipid vesicles) or binary (comprising two type of alcohols). Ethanol injection was employed for vesicles preparation, and sodium alginate, as gelling agent. We purposed the local-transdermal administration of the off-the-shelf retinoid fenretinide (FENR) for chemoprevention of breast cancer. Rheograms and flow index values for alginate dispersion (without ethosomes) and hydrogels containing simple, mixed or binary ethosomes suggested pseudoplastic behavior. An increase in the apparent viscosity was observed upon ethosome incorporation. The ethosomal hydrogel displayed increased bioadhesion compared to the alginate dispersion, suggesting that the lipid vesicles contribute to the gelling and bioadhesion processes. In the Hen's Egg Test–Chorioallantoic Membrane model, few spots of lysis and hemorrhage were observed for formulations containing simple (score of 2) and mixed vesicles (score 4), but not for the hydrogel based on the binary system, indicating its lower irritation potential. The binary ethosomal hydrogel provided a slower FENR *in vitro* release and delivered 2.6-fold less drug into viable skin layers compared to the ethosome dispersion, supporting the ability of the gel matrix to slow down drug release. The ethosomal hydrogel decreased by ~ five-fold the IC_{50} values of FENR in MCF-7 cells. In conclusion, binary ethosomal gels presented technological advantages, provided sustained drug release and skin penetration, and did not preclude drug cytotoxic effects, supporting their potential applicability as topical chemopreventive systems.

Keywords Nanomedicine · Retinoid · Bioadhesion · Transdermal hydrogel

INTRODUCTION

The synthetic retinoid fenretinide (FENR) is a promising active agent for prevention of breast cancer development and recurrence due to encouraging findings in clinical trials, such as its ability of accumulation in the breast tissue, tolerability during longer-term use and inhibition of mammary carcinogenesis (1). However, FENR poor aqueous solubility and low availability have hindered its clinical use (2). These issues can be addressed by the development of formulations based on nanotechnology (3) and use of alternative routes, such as topical delivery directly to the breast skin (4).

Nanocarriers are recognized for increasing the apparent solubility and bioavailability of lipophilic compounds (5). They can also improve drug transport across biological barriers like the skin, enabling local-transdermal therapy (LTT) (3). In the LLT approach, the drug is applied directly on the

✉ Alexsandra Conceição Apolinário
acapolinario@usp.br

✉ Luciana Biagini Lopes
lublopes@usp.br

[1] Department of Pharmacology, Institute of Biomedical Sciences, University of São Paulo, Av. Prof. Lineu Prestes, 1524, São Paulo, SP 05508-000, Brazil

[2] Centre of Excellence in New Target Discovery (CENTD), Butantan Institute, São Paulo, Brazil

[3] School of Pharmaceutical Sciences, São Paulo State University (UNESP), Araraquara, São Paulo, Brazil

breast skin, improving its concentrations in the mammary tissue and providing a more localized approach to avoid the development and recurrence of breast cancer lesions (3, 6, 7). Among many nanocarriers, liposomes have attracted attention for their multiple advantages. They enable compartmentalization of hydrophobic drugs in the bilayers, leading to increased apparent solubility, as well as accommodation of hydrophilic drugs into the aqueous compartment, allowing the co-encapsulation of molecules with varying physicochemical properties. These nanovesicles are biocompatible and have been approved for clinical use (8). Additionally, they can be modified with surfactants and solvents that act as skin penetration enhancers (9), leading to new terminologies according to composition and performance. For instance, ethosomes refer to liposomes that comprise up to 50% of ethanol (10), while addition of surfactants and propylene glycol to ethosomes originate mixed and binary systems (11). The development of ethosome-based hydrogels (e.g. ethosomal gel) is promising for combining the advantages of ethosomes with the benefits of gel formulations including bioadhesion and easy application to the skin (12).

Herein, we hypothesized that the addition of sodium alginate to the ethosomes would produce a semisolid system in a similar manner to calcium chloride crosslinking, enabling obtainment of a hydrogel in the presence of vesicles. Thus, the ethosomal hydrogel would allow the entrapment and delivery of hydrophobic drugs like FENR in a predominant aqueous semisolid formulation. We developed a sodium alginate-based hydrogel to incorporate three different types of FENR-loaded ethosomes aiming LLT to prevent breast cancer development and recurrence in patients previously subjected to surgery. We employed the ethosomal technology described in our previous work (11) to obtain an ethosomal hydrogel with enhanced viscosity, bioadhesion and prolonged release profile compared to simple dispersions of alginate or ethosomes. We compared the physicochemical characteristics and irritation potential of the hydrogels based on simple, mixed and binary ethosomes and, after formulation optimization, assessed their ability to increase penetration of FENR into different skin and to reduce the viability of breast cancer cells.

MATERIALS AND METHODS

Materials

Soybean lecithin (mixture with 97.2% phosphatidylcholine and 2.8% of lysophosphatidylcholine, MW = 775.037 g/mol), Tween 80® (polyoxyethylene sorbitan monooleate, 1.310 g/mol and critical micelle concentration $\approx 1.2 \times 10^{-5}$ mol/L), propylene glycol (MW = 76.09 g/mol) and phosphate-buffered saline tablets were obtained from Merck (St. Louis, MO, USA). Fenretinide (FENR) was obtained from Cayman (391.37 g/mol, Ann Harbor, MI, PA, USA). Other reagents include rhodamine B (MW = 479 g/mol, Synth, Diadema, São Paulo, SP), sodium alginate medium viscosity (1% aqueous solution at 25 °C ~ 600–900 cps, MP Biomedicals, Santa Ana, CA, USA), ethanol (Coperalcool, Barueri, SP, São Paulo), HPLC grade acetonitrile (Honeywell, Morristown, NJ, USA) and ultrapure water (resistivity of 18 MΩ cm^{-1} at 25 °C, Millipore, Bedford, MA, USA).

Preparation of Ethosomes and Ethosomal Hydrogel

Ethosomes were developed using a previously reported method, which is based on the quality by design approach and ethanol injection (11). The lipid phase was composed of ethanol at 20 (for binary ethosomes) or 30% v/v (for simple ethosomes), lecithin (2%, w/v) and fenretinide (to provide a final concentration of 2.5 mg/mL). More specifically, for simple ethosomes, this phase consisted of ethanol and lecithin, while ethanol and propylene glycol (at 20:10 v/v) were mixed with lecithin (2%) for binary vesicles (11). In the case of mixed vesicles, a dispersion of Tween 80 above CMC (resulting in a final concentration of 2%) was employed as an aqueous medium. The organic phase was pumped at 100 µL/min into the aqueous medium (KD Scientific Syringe Pump, Holliston, MA, USA), and the system was stirred for 30 min at 300 rpm.

To prepare the ethosomal hydrogels, a one-step method was carried out: sodium alginate was added to the various ethosome dispersion (2% w/v), and the system was centrifugated for 5 min to enable complete homogenization and gelling (1000 × g for 5 min). Alginate dispersions were used as control, which were produced by adding sodium alginate (2% w/v) to purified water without addition of any crosslinking agent. Optical microscopy analysis was performed to examine the presence of drug crystals.

Ethosome Physicochemical Characterization

For ethosome characterization, the hydrodynamic diameter, polydispersity index (PDI) and zeta potential were measured at 25 °C using a Malvern Zetasizer Nano ZS90 instrument (Malvern Instruments Ltd., UK) after sample dilution with filtered ultrapure water (0.45-µm filter) at 1:20 (v/v). They were placed in polystyrene cuvettes for determination of the hydrodynamic diameter or in glass cuvettes equipped with dip cell (Malvern Instruments Ltd., UK) for zeta potential evaluation. Three individual measurements of each ethosome batch (3) were conducted, and the results were expressed as the average of these measurements.

The ethosomal hydrogel and the alginate dispersion were also diluted at the same ratio in water and in DMEM-F12 (Dulbecco's Modified Eagle Medium/Nutrient Mixture F-12) containing 10% heat inactivated fetal bovine serum to investigate the influence of the gel network and cell culture medium on size distribution.

Rheological behavior of the ethosomal hydrogels

To evaluate the rheological behavior of the ethosomal hydrogels, a cone and plate rheometer (RST-CPS Cone/Plate equipped with Rheo3000 software, Brookfield, Middleboro, MA) was employed. Samples were maintained at 32 °C, and shear rates were gradually increased and subsequently decreased in the range of 0–2000s^{-1}. Plots showing variations in the shear stress or viscosity as a function of the shear rate were obtained to evaluate the rheological behavior, while the Power law equation was employed for determination of the flow index as described in a previous study (38).

$$\tau = K\gamma^n \quad (1)$$

In which: τ = shear stress, γ = shear rate, k = consistency index and n = flow index.

The alginate dispersion(obtained at 2%, w/v) was employed as control formulation.

Irritation Potential Screening

The Hen's Egg Test–Chorioallantoic Membrane (HET-CAM) model was employed for estimation and comparison of the irritation potential of the ethosomal hydrogels. In brief, fertilized chicken eggs were acquired from Yamaguishi Orgânicos (Campinas, SP, Brazil). They were incubated for 9 days at 37 °C and 55% humidity (Premium Ecologica, Belo Horizonte, MG, Brazil). After cutting the shell and exposing the membrane, 100 mg of the test formulations or control solutions (NaCl 0.9% and NaOH 0.1 M as negative and positive controls, respectively) maintained at room temperature (to avoid constriction) was gently applied. Each treatment was performed in 3–5 eggs. Before application and at 30, 60, 120, 180, 240 and 300 s post-application, the membranes were assessed and photodocumented for the occurrence of endpoints of coagulation, lysis and/or hemorrhage.

The irritation index was calculated using the following equation:

$$II = \left(\left(\frac{301-h}{300}\right)x5 + \left(\frac{301-l}{300}\right)x7 + \left(\frac{301-c}{300}\right)x9\right) \quad (2)$$

In which: h, l and c are the time (in seconds) of the beginning of hemorrhage, lysis or coagulation. The following classification was used as previously described: 'II < 0.9: not labeled; 1.0 < II < 4.9: slightly irritating; 5.0 < II < 8.9: moderately irritating; 9.0 < II < 21: severely irritating' (13).

In Vitro Fenretinide Release from the Ethosomal Hydrogel and Ethosomes

To assess the ability of the alginate polymeric matrix to provide a slower drug release compared to the ethosomes, FENR release was investigated for 48 h. Samples were placed in cell culture inserts (12 mm of diameter, 1.12 cm^2 of membrane diffusion area and pore size of 1 µm) (14), and the inserts were positioned in 12 well plates containing 3 mL of PBS (pH ~ 7.4) with 1% polysorbate 80 (to improve drug solubility), which was employed as receptor phase for this and the skin penetration studies to maintain the similarity between the receptor phases in these experiments (15–21).

One hundred microliters of ethosomes and 100 mg of ethosomal hydrogel were employed. Using 100 µL of ethosomes yields an average of 98 mg hydrogel. For simplification and by approximation, this volume was considered equivalent to 100 mg of the dispersion. The plates were stirred at 50 RPM for 48 h, and aliquots (500 µL) of the receptor phase were collected and replaced at 30 min, 1, 2, 3, 4, 5, 6, 7, 8, 12, 24, 48 h. The concentration of the drug released at each time point was assessed using a SpectraMax Absorbance Microplate Reader (Molecular Devices, São Paulo, SP, Brazil) set at λ = 365 nm. A calibration curve of the pure drug in tween 80 at 1% (w/v, 0.5–100 µg/mL) was employed. Linearity was observed from 0.5 to 20 µg /mL and the limit of quantification of 0.5 µg/mL. The cumulative percent release of FENR as a function of time t was calculated according to the equation:

$$P_t(\%) = \frac{M_t}{M_0}.100 \quad (3)$$

In which: M_t is the cumulative absolute amount of fenretinide released at time t during releasing assay (corrected for drug amounts that were withdrawn at previous time points) and M_0 the absolute amount of drug within the ethosomal hydrogel or ethosome dispersion at the beginning (t = 0).

To study the mechanism of FENR release, equations for zero-order, Higuchi square root and Hixson were employed for data fitting, and the coefficients of determination were obtained (Origin Lab Corporation, Wellesley Hills, MA, USA). The zero-order release model is represented in Eq. 4 (22):

$$\frac{M_t}{M_\infty} = k_0 t. \quad (4)$$

In which: k_0 is the zero-order kinetic constant, calculated as the slope of the plot representing the relationship between

cumulative FENR release and time. M_t is the cumulative absolute amount of fenretinide released at time t during releasing assay (corrected for drug amounts that were withdrawn at previous time points) and M_0 the absolute amount of drug within the ethosomal gel or ethosomal system at the beginning ($t=0$).

The Higuchi model is simplified in Eq. 5 (23):

$$\frac{M_t}{M_\infty} = k_H\sqrt{t} \tag{5}$$

In which: k_H is the Higuchi constant.

Drug release mediated by dissolution and change in the carrier surface area and diameter is described by the Hixson-Crowell model according to Eq. 6:

$$Q_0^{\frac{1}{3}} - Q^{\frac{1}{3}} = K_{HC}t \tag{6}$$

In which: Q is the FENR % residual in matrix at time, t, and K_{HC} is the Hixson-Crowell constant.

In Vitro Bioadhesive Properties

The bioadhesion assay was adapted from Fonseca-Santos *et al*. (24). Samples were weighted (~2.0 g) in 5-mL polypropylene microcentrifuge tubes, which were centrifuged at 2000 × g for 2 min to eliminate bubbles and left to rest for 24 h prior to the assay. Pieces of porcine ear skin were incubated with 0.9% NaCl solution prior to analysis for hydration and cut with a hollow punch cutter ($d=10$ mm) to obtain circular sections. The skin sections were fixed in a cylindrical probe ($d=10$ mm) covered with tape for protection, which was placed in the arm of TA.XT plus texture analyzer (Stable Micro Systems, Surrey, UK, Figure S1). The formulations were placed in a water bath (32 °C), and the probe was lowered at 5 mm/s until penetrating the formulation (depth of 1 mm), where it was maintained for 60 s. Subsequently, the probe was raised at 5 mm/s, and the detachment force was recorded and compared among the various test formulations.

Evaluation of Skin Penetration and Distribution

Comparison of the Influence of Ethosomal Gels on the Penetration of FENR

Skin penetration studies were performed in Franz diffusion cells (permeation area of 0.67 cm^2, Hanson, Chatsworth, USA) (11). Skin sections removed from the outer surface of porcine ears were dermatomed (TCM 3000 BL, NOUVAG, Zurich, Switzerland) at 1 mm, and placed on the top of diffusion cells with the dermis facing down to the receptor phase, composed of PBS with pH ~ 7.4 containing Tween 80 at 1% (w/v), and kept under magnetic stirring (350 RPM) at 32 °C. The skin surface (which was facing up) was treated for 24 h with 100 mg of the various ethosome gels, 100 µL of ethosome dispersions (for comparison) or 100 µL of the control solution (drug in propylene glycol) as previously described (25, 26).

After the 24-h treatment, the setup was disassembled, and the skin sections and receptor phase of each cell were collected for FENR extraction and quantification. The surface of each skin section was gently rinsed with distilled water, blotted dry with paper tissue, and the *tape stripping* technique was employed to separate the *stratum corneum* (SC) from the remaining skin layers (which will be referred to as viable skin or epidermis without *stratum corneum* + dermis). In this technique, the SC of the permeation area was removed by the application and quick removal of 15 sequential adhesive tape strips. With the exception of the first tape, all others were subjected to FENR extraction using methanol, vortex mixing and bath sonication (Quimis, Diadema, SP, Brazil, 20 min) (11).

After tape stripping, the remaining skin was cut in small pieces, subjected to homogenization (Biospec Products, Bartlesville, OK, USA) with methanol and bath sonication (Quimis, Diadema, SP, Brazil) for 20 min (11). All samples were filtered prior to FENR quantification. The receptor phase (RP) was also subjected to filtration for FENR quantification and determination of transdermal delivery or percutaneous permeation, which estimates the amount of FENR that could reach the circulation.

FENR delivery to the skin and receptor phase was quantified by high-performance liquid chromatography (HPLC) according to a method previously developed (11) using a Shimadzu HPLC system consisting of a pump (LC-20AB), autosampler (SIL-20A) and a photodiodoarray detector (SPD-M20A) set a 340 nm. A Phenomenex C18 column (at 25 °C) was employed for separation using acetonitrile:water:acetic acid (80:17:3 v/v/v) at 1 mL/min as mobile phase. The quantification limit was 0.1 µg/mL; linearity was studied between 0.1 and 5 µg/mL with an R^2 of 0.9984.

Visualization of Ethosomal Gel-Mediated Penetration by Confocal Laser Scanning Microscopy

As proof of concept that ethosomes favor drug penetration, skin sections were also treated with a dispersion of binary ethosomes containing rhodamine B (0.25%) as model hydrophobic drug, and the dye distribution in the skin was assessed using confocal microscopy. Treatment with an isopropyl myristate solution of the dye was performed as control. After 6 h of treatment, the skin surface was gently rinsed and blotted dry with paper tissue. Following, a foam tape was used to fix the skin on the glass slides, and the

tissues were scanned on the x, y and z axis using a confocal microscope with a 5×/0.15 objective lens and laser excitation at 552 nm (TCS SP8, Leica microsystems). The acquisition of images, quantification of the fluorescence intensity of the z-stack profile and 3D reconstruction were performed using the LAS X software in the respective modules (Leica microsystems).

Cytotoxicity of the Ethosomal Gel

The effect of the gels on the viability of breast cancer cells was assessed using MCF-7 cells (ATCC® HTB-22™) and MTT assay (27). The cells were cultivated with DMEM-F12 medium supplemented with heat inactivated FBS (10%) and antibiotics (100 U/mL penicillin, 100 µg/mL streptomycin) in T-25 cm^2 cell culture flasks. Culture conditions included temperature of 37 °C, CO_2 at 5% CO_2 and 95% humidity (28).

For assessment of the influence of the gels on viability, MCF-7 cells were seeded at 1×10^5 cells/mL in 96 well plates and treated with serial dilutions of FENR solution in DMSO (0.3–20 µM final concentration in the cell culture medium) or FENR-loaded ethosomal gels (for 0.3–20 µM fenretinide concentration in the medium). After 48 h, treatment was replaced by the MTT reagent (5 mg/mL), followed by an additional incubation for 3 h to allow the conversion of the reagent into the purple formazan derivative by viable cells. The derivative was subsequently extracted using dimethyl sulfoxide, and absorbance was recorded at 570 nm. The results were reported as means ± standard deviation (SD) a minimum of three independent experiments, with 3 wells for each treatment in each experiment. Untreated cells were used as control, and the percent cell viability was determined using the formula below:

$$Cell\ viability_{\%} = \frac{A_{\text{test}}}{A_{\text{control}}} \times 100 \quad (8)$$

In which, A_{test} is the absorbance of the test solution and A_{control} is the absorbance of the control. GraphPad Prism was used to calculate the 50% inhibitory concentrations (IC_{50} values).

Statistical Analyses

Results were expressed in plots and/or tables as means ± standard deviation (SD). Data analysis was conducted using GraphPad Prism 6.01 (GraphPad Software Inc., La Jolla, USA) for one-way analysis of variance (ANOVA) followed by Tukey post hoc test; statistically significant differences were detected when $p < 0.05$.

RESULTS AND DISCUSSION

Ethosomal Gel Obtainment and Characterization

We obtained three ethosomal systems according to the methodology previously developed by our group (11): (1) ethosomes based on lecithin and ethanol, which were referred to as simple ethosomes, (2) mixed systems, composed by two types of nanostructures in the same system, i.e. vesicles and micelles of Tween 80; and (3) binary vesicles, composed by the blend of two types of alcohols (ethanol:propylene glycol).

The vesicles may coexist with cosolvents, micelles and/or surfactants monomers, which can influence the solubility of FENR and other hydrophobic drugs in vesicle dispersions and their medium (3, 11). Thus, we did not separate the non-encapsulated and encapsulated FENR but instead worked with the concept of drug incorporation, which corresponds to the fractions of FENR encapsulated in the ethosomes and homogeneously dissolved/dispersed in the medium. This was possible because there were no drug pellets/crystals in the formulation, and 100% of the drug concentration added to obtain the ethosomes (final concentration of 2.5 mg/mL) remained incorporated in the dispersion and, subsequently, in the hydrogel. From the total drug incorporated, we had previously estimated that 50% should be within the ethosomes (3, 11). Thus, based on this approach, it was possible to incorporate 100% of the added FENR content in a predominantly aqueous semisolid formulation.

The ability of these nanoformulations to deliver FENR to the skin has been previously demonstrated (11); building upon this work, here we assessed an ethosomal hydrogel that can be directly applied to the skin. A classical gel generally presents less than 10% of polymer, which forms a substantial solid–liquid interfacial area within the gel. They are classified according to the kind of liquid phase: organogels, comprising organic solvent and hydrogels containing water (29). A conventional hydrogel is generally defined as a system formed by crosslinked 3D networks of hydrophilic polymer chains that present the ability to swell and retain a significant fraction of water within its structure without dissolving (30, 31). The crosslinks can be constituted of entanglements, crystallites, covalent bonds or other types of interactions (such as hydrogen bonding, solvophobic, charge transfer and van der Waals) (29).

Herein, ethosomal hydrogels were developed using sodium alginate (Na-Alg), a sodium salt of alginic acid, as gelling agent (25). Sodium alginate has been demonstrated to self-aggregate and to undergo gelation and cross-linking forming hydrogels by the exchange of sodium ions with divalent cations (Afshar *et al.*, 2020). However, here we

observed that gelling occurred upon the addition of alginate to ethosomes with negative zeta potential. Mean zeta potential values were − 27 (± 0.05), − 15 (± 0.1) and − 29 (± 0.9) mV for simple, mixed and binary ethosomes, respectively. Our findings are supported by previous reports indicating that gel networks of negatively charged polymers (such as alginate) can be reinforced by their interaction with lipid vesicles (32). In the absence of divalent cations to promote crosslinking, other theories might explain the interaction between lipids (e.g. phosphatidylcholine used for ethosome obtainment) and negatively charged polysaccharides. Phospholipids could interact with negative polymers by competing for the hydrophobic regions along the polymer (32, 33). Additionally, hydrogen bound formation could offer an additional explanation for their interactions (34).

We also investigated whether ethosomes physicochemical characteristics were altered upon their incorporation in the alginate hydrogel. In the DLS graphs (Fig. 1A–C), it was possible to observe size populations that suggest the presence of ethosomes (200 nm for simple ethosomes, 220 nm for mixed ethosomes and 580 nm for binary ethosomes) after gelling with sodium alginate, which supports the maintenance of the ethosome structural organization after the gelling process. A population consistent with micelles was also observed when the mixed systems were analyzed by number distribution (instead of intensity) (Fig. 1B, inset). Additionally, particle sizes relatively large for vesicles were also observed after the gelling process, most likely due to limitations of the light scattering technique, since the presence of polymer chains could disturb Brownian moving.

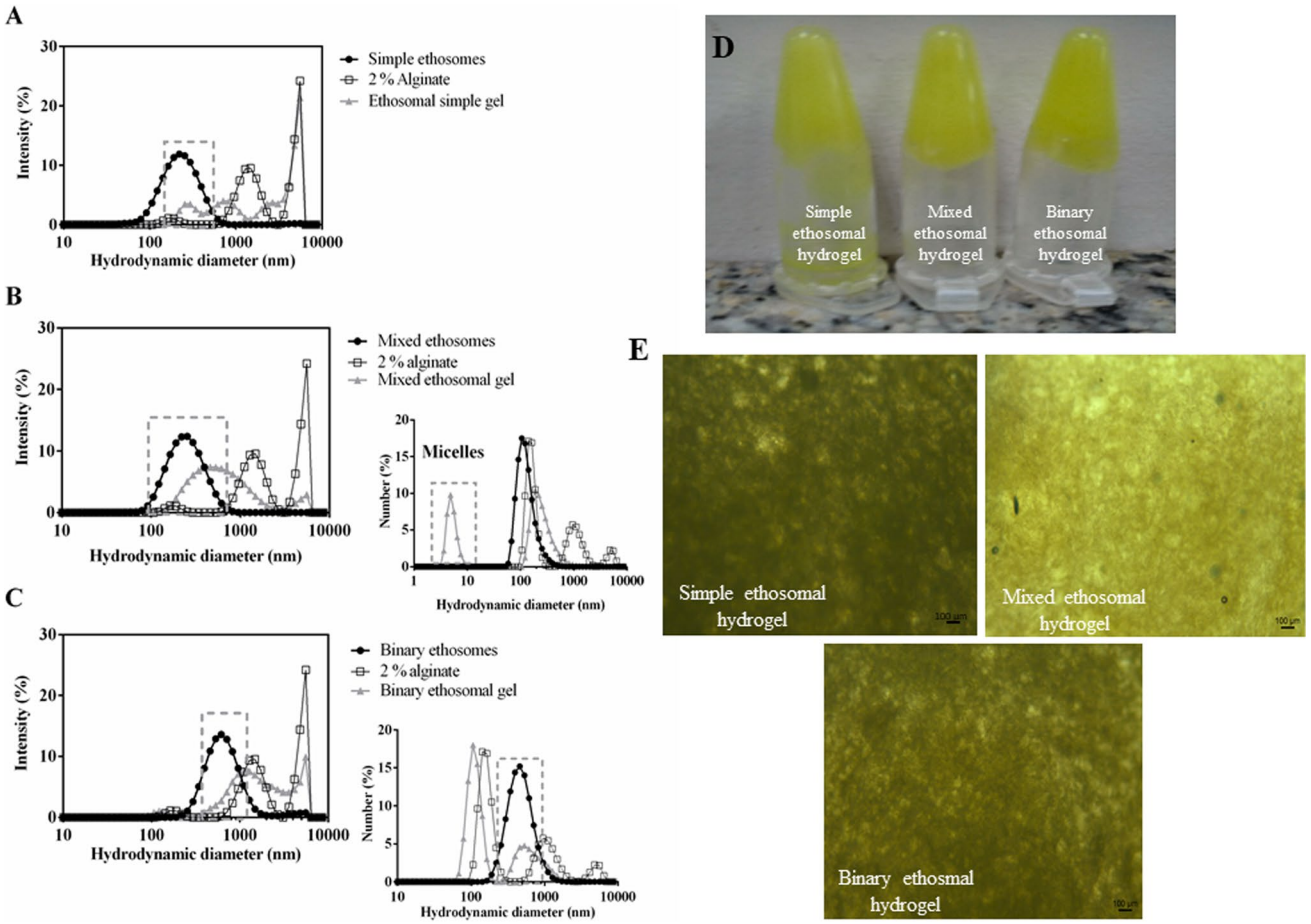

Fig. 1 Characterization of the ethosomal hydrogels. In panel **A**, **B** and **C** is depicted the hydrodynamic diameter distribution of simple, mixed and binary ethosomes, respectively, as dispersions and their respective hydrogels; the unloaded 2% alginate dispersion was used for comparison. In each panel, for intensity distribution, the gray dotted squares indicate the common size ranges (red and black lines) suggesting the presence of ethosomes after the gelling process. The number distribution profile of size highlights the presence of a micelle population in mixed systems and the common peaks of size for binary ethosomes, which was not clear by the size distribution analyzed by intensity. Panel **D** shows the macroscopic appearance of the ethosomal hydrogels, which presented homogeneity without signals of drug precipitation. Panel **E** depicts the optical microscopic images of the ethosomal hydrogels indicating absence of drug crystals and full solubilization of fenretinide

All formulations were macroscopically homogeneous, indicating a successful gelation even in the absence of cations (Fig. 1D). No drug crystals were observed under the microscope (Fig. 1E), indicating solubilization of the hydrophobic FENR in the aqueous hydrogel. This finding is relevant since, as already mentioned, the ethosomal systems encompass both encapsulated and dissolved/dispersed FENR (11); dissolving the highly hydrophobic FENR in hydrogels without ethosomes would be unlikely. Because drug pellets or insoluble crystals were not visualized, it is reasonable to assume that any non-encapsulated drug fraction was solubilized or well dispersed in the system. Such finding is rather promising since, in most studies, the free (non-entrapped) drug is removed from the dispersion and, thus, wasted (35).

Rheological Behavior of the Ethosomal Hydrogels

Rheological measurements demonstrated that the relationships between shear stress and shear rate were not linear (Fig. 2A), indicating that all formulations displayed non-Newtonian behavior. The pseudoplastic behavior was suggested by the viscosity decrease as the shear rate gradually increased (Fig. 2B) and by the values of the calculated flow indices, which were less than unity for all samples. More specifically, values of 0.58, 0.32, 0.36 and 0.32 for conventional (without ethosomes) alginate dispersion, simple, mixed and binary ethosomal hydrogels, respectively, were obtained. Newtonian behavior is observed when $n = 1$, while shear-thickening and shear-thinning behaviors are indicated by $n > 1$ or $n < 1$, respectively. The flow resistance of pseudoplastic gels is low when it is applied under medium to high shear conditions, so this rheological behavior is ideal for application of formulations on the skin. This type of behavior can be justified by the alignment of vesicles/aggregates in the direction of the flow (14).

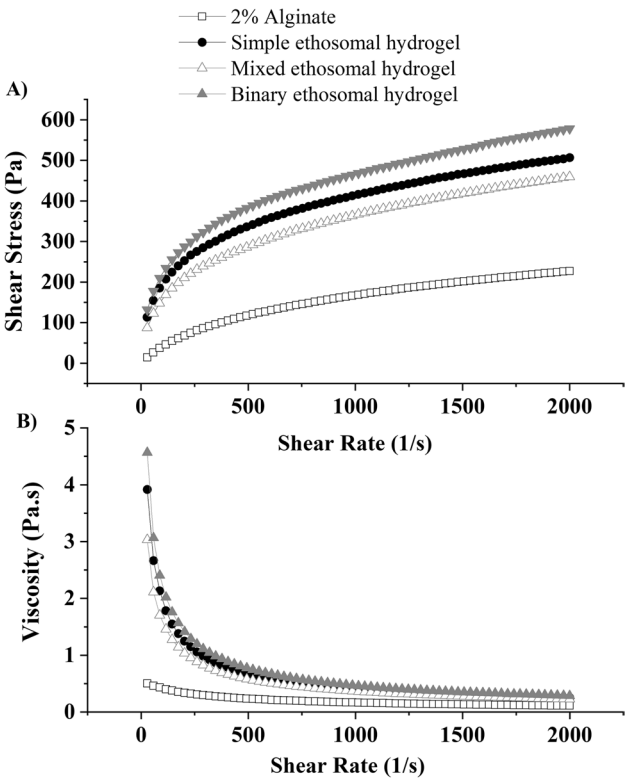

Fig. 2 Rheological behavior (**A**) and apparent viscosity (**B**) of the simple, mixed and binary ethosomal hydrogels in comparison to the 2% alginate dispersion (without ethosomes). Flow indices calculated were 0.58, 0.32, 0.36 and 0.32 for 2% alginate dispersion, simple, mixed and binary ethosomal hydrogels, respectively. The reduction of viscosity along the gradual increase of the shear stress and the flow index < 1 is consistent with pseudoplastic rheological behavior

All ethosomal hydrogels displayed higher viscosity values at lower shear rates (up to 500 s^{-1}) than the alginate dispersion, indicating that the vesicles contribute to the formation of the hydrogel. Among the ethosomal hydrogels, the formulation based on mixed ethosomes presented lower viscosity, while higher viscosity values were observed for the binary ethosomal hydrogel. For instance, at a shear rate of 361 s^{-1}, the viscosity values of simple, mixed and binary hydrogels were 1, 0.8 and 1.20 Pa s, respectively; a viscosity value of 0.3 Pa s at the same rate of shear was found for the alginate dispersion without ethosomes. Devi and Karati (2013) (36) reported that gelling is prevented in the presence of Tween 80; herein, although we were able to obtain a gel-like system with the presence of mixed ethosomes, the viscosity was the lowest among the ethosomal hydrogels.

We also observed a relationship between vesicle size and viscosity, with higher sizes observed in hydrogel with higher viscosity. The size of binary ethosomes was ~ 500 nm, while simple and mixed vesicles presented size around 200 nm. Size changes were associated with modification of ethosome composition (11) and agree with previous reports: presence of a micelle population in the system composed of mixed vesicles and the combination of ethanol and propylene glycol in binary ethosomes have been reported to increase the size of vesicles (37). However, contrary to our observations, El Kechai *et al.* (2015) (32) reported that vesicle size increases and consequent reduction of the surface area affects interactions that control the rheological properties of alginate hydrogels.

Overall, the rheological proprieties of ethosomal hydrogel demonstrated technological advantages and indicated enhanced performance of binary ethosomal-based gel compared to the simple alginate dispersion in water.

Irritation Potential Screening

The HET-CAM model is widely applied for ophthalmic products and has been successfully extrapolated for skin irritation investigation (38, 39). In this model, if the formulation

causes no vascular alterations, it is assumed that it would not cause skin irritation. Although alginate is considered a biocompatible and non-irritant material with wide biomedical applicability, the potential of the hydrogels to cause irritation was studied to evaluate whether the presence of nanovesicles with varied composition affected the overall formulation safety. Images of the membranes after removal of the formulations and the scoring results are shown in Fig. 3. The positive control, i.e. NaOH, caused lysis and hemorrhage; its score of 10.8 justifies its classification as severely irritating. Negative control (saline) did not cause irritation. Few spots of lysis hemorrhage were observed for simple and mixed hydrogels, resulting in scores of 2 and 4, respectively, indicating that they are slightly irritating. For the hydrogel based on binary ethosomes, the endpoints lysis, hemorrhage and coagulation were not detected, indicating that this ethosomal hydrogel is non-irritant.

These differences in irritation can be associated with composition. According to the list of *Inactive Ingredients from Approved Drug Products* from Food and Drug Administration (FDA), the maximum concentration of Tween 80 for ophthalmic products is 0.05% w/v, which is 20-fold lower than the concentration in the hydrogel, which thus, limits the application of the HET-CAM model for irritation potential estimation of the mixed hydrogel. The slight irritation observed for simple ethosomes compared to the binary systems could be explained by the higher ethanol concentration in the former. Propylene glycol, added to the binary system to replace 10% of the ethanol content, is approved for use up to 15% w/w in ophthalmic formulations and up to 30% w/w for topical application. Since its concentration in the hydrogel is within this limit, the formulation could be considered safer (40). Based on the higher viscosity and non-irritant properties, the hydrogel based on binary ethosomes was selected for further studies.

In Vitro Fenretinide Release

Figure 4 compared *in vitro* FENR release from the binary ethosome system and the ethosomal hydrogel containing binary ethosomes. Since we worked with the concept of 'drug incorporation' as previously discussed, and

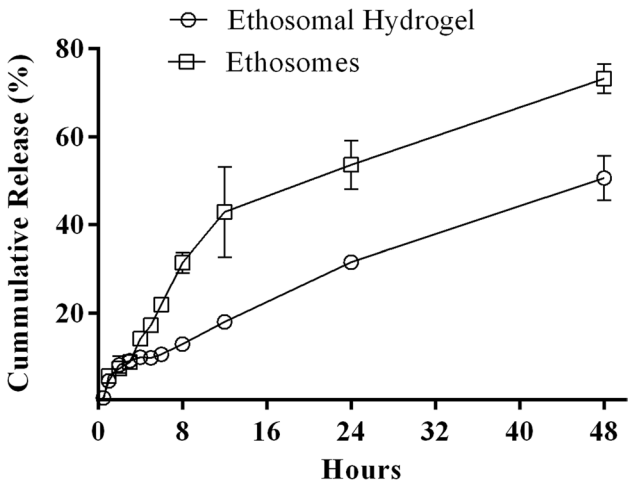

Fig. 4 Cumulative release of fenretinide from the binary ethosomes and from the ethosomal hydrogels containing binary ethosomes as a function of time

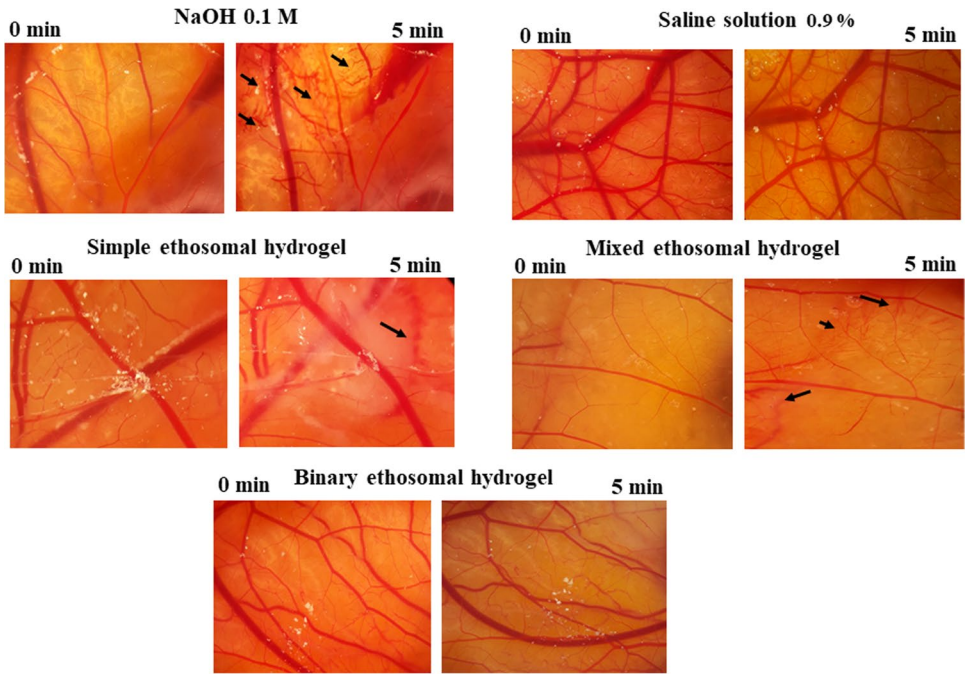

Fig. 3 Irritation potential of ethosomal hydrogels evaluated according to the Hen's Egg Test–Chorioallantoic Membrane (aptHET-CAM) model as changes on CAM after exposure to the hydrogel, saline 0.9% (negative control) or NaOH (0.1 M, positive control) for 5 min. The black arrows indicate areas of hemorrhage in the membrane. The positive control (NaOH) is severely irritating leading to lysis and hemorrhage, resulting in a score of 10.8. Simple and mixed ethosomal hydrogels were slightly irritating (scores of 2 and 4, respectively), since only some spots of lysis hemorrhage were observed. Binary ethosomal hydrogels were considered non-irritant

considering that the ethosomal hydrogel incorporated 100% of the FENR amount added (final concentration of 2.5 mg/mL), both the drug-loaded ethosomes and drug-loaded ethosomal gel compared here contained the same amount of FENR. As expected, FENR release from the ethosomal hydrogel was lower. At 8 h, the hydrogel released around 13% of the drug content compared to 31% released from the ethosome dispersion. At 48 h, the hydrogel released ~ 50% of the drug compared to ~ 73% released from the ethosome dispersion. The results of data fitting using selected kinetics models are depicted in Table I.

Release and diffusion of water-insoluble drugs from hydrogels can be explained by erosion of the outer gel layer as it becomes well hydrated (41). In the first 8 h and from 8 to 48 h, FENR release from the ethosomal hydrogel can be best described by the Higuchi model ($R^2 = 0.9294$ for release from 0 to 8 h and 0.9996 for release from 8 to 48 h), which is applicable when release is largely controlled by diffusion through water-filled pores in a matrix (42). Therefore, our data suggest that FENR diffusion through the matrix plays an essential role in its release. The Higuchi's square root model implied a biphasic pattern, in which a slower-release pattern follows an initial burst release. The degradation rate of the ethosomal hydrogel might become faster with time, producing defects in the matrix and enabling a faster diffusion process. The second-best model to describe release was the Hixson-Crowell model, which confirmed the influence of matrix erosion on the FENR diffusion through it, especially after 8 h. For the Hixson model, drug release is presumed to be limited by the dissolution velocity, which can happen through the polymeric matrix (43).

Our findings agree with reports involving drug release from gels based on vesicles. For instance, clove oil release from the ethosomal gel based on Carbopol 974 followed the Higuchi model (44). Release of lidocaine from liposomal hydrogels based on Carbopol 940 was also in accordance with the Higuchi model (45). Drug release from liposome gels produced with Pluronic® F-127 displayed the highest R^2 for the Higuchi model (46).

In contrast to the ethosomal hydrogel, FENR release from the ethosome dispersion followed zero-order kinetics in the first 8 h ($R^2 = 0.9812$) and the Hixson-Crowell model from 8–48 h ($R^2 = 0.9852$), both models resulting in higher R^2 values than the Higuchi model ($R^2 = 0.9846$). The zero-order kinetics model has also been associated with drug release of lipid vesicles and indicates that drug release occurs as a function of time and that the process takes place at a constant rate that does not depend on drug concentration. This is appropriate for prolonged release and transdermal delivery, and includes matrix, coated and osmotic systems matrix (43). These findings suggest that the ethosomal bilayer might act as a barrier to FENR partition and release by diffusion (47), and are in accordance with other studies that report zero-order kinetics and suggest that ethosomes might act as reservoir systems (45).

Table I Coefficient of Determination (R^2) Calculated After Release Data Fitting to Selected Kinetics Models

Models	Ethosomal hydrogel (0–8 h)	Ethosomal hydrogel (8–48 h)	Ethosomes (0–8 h)	Ethosomes (8–48 h)
Zero order	0.8163	0.9903	0.9812	0.961
Higuchi	0.9294	0.9996	0.8761	0.9846
Hixson	0.8242	0.9975	0.9737	0.9852

In Vitro Bioadhesive Properties and Comparison of the Influence of Ethosomal Hydrogels on the Skin Penetration of FENR

Bioadhesion refers to a phenomenon that maintains two materials (one of them is biological, such as the skin) together by interfacial forces for an extended period of time (48). This is an important feature for topical administration to the skin, as it improves drug residence time at the absorption site, leading to an enhanced contact with the skin barrier, which can decrease the frequency of formulation application and increase patient compliance (49).

Since the ethosomes increased viscosity even in the absence of divalent ions, we assessed whether their presence affected the bioadhesive properties compared to the alginate dispersion (2% m/v) in water. As can be observed in Fig. 5A, the presence of ethosomes led to a ~ 2 × -fold ($p < 0.05$) increase in the force of adhesion compared to alginate dispersion and threefold compared to water. Alginate is formed by 1,4-linked b-D-mannuronate and 1,4-linked a-L-guluronates residues, and its bioadhesion potential has been attributed to the carboxyl groups and formation of hydrogen bounds with sialic acid residues in the skin (50). Due to the influence of viscosity on bioadhesive properties, these findings might be related to the higher viscosity of the ethosomal-based hydrogel compared to alginate dispersion (51). Figure 5B depicts an image of pig ear skin treated with gel after 24 h of application showing that the formulation still adhered to the tissue. Such enhanced performance of the binary ethosomal hydrogel is an additional advantage for LTT and breast cancer chemoprevention.

Both ethosome dispersion and ethosomal hydrogel delivered FENR into the skin (Fig. 6). The amount of FENR delivered in the *stratum corneum* (SC) by the ethosomal hydrogel was 1.7 and threefold smaller compared to the ethosome dispersion and the control solution in isopropyl myristate, respectively. As can be observed in Fig. 6B, after few hours of treatment, the ethosomal hydrogel forms a film on the skin surface, most likely due to evaporation of water. This film could be removed from

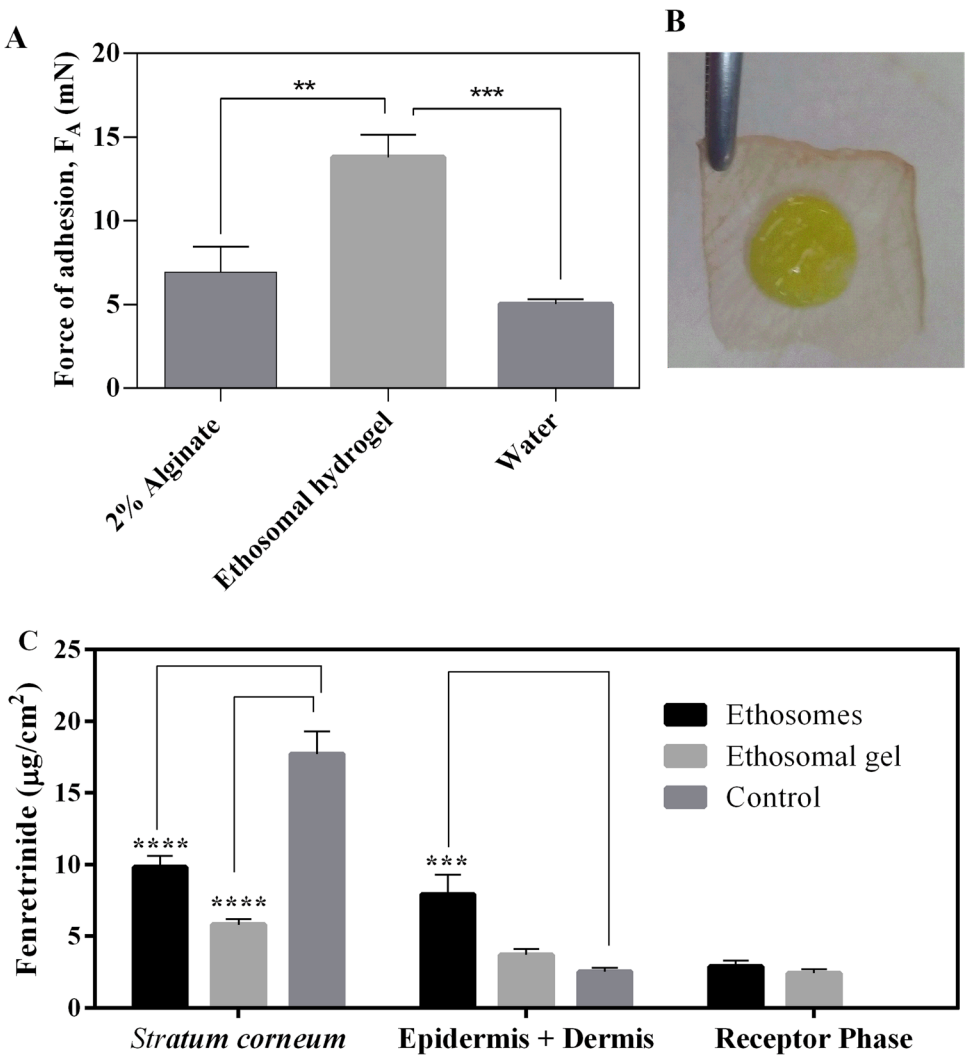

Fig. 5 Bioadhesive properties and skin penetration of fenretinide (FENR). **A** *In Vitro* bioadhesive potential comparing the maximum peak force of detachment of water (control), the 2% alginate dispersion and ethosomal hydrogels. **B** Image of the ethosomal hydrogel on pig ear skin after 24 h of treatment. *** $p < 0.001$ compared water and ** $p < 0.005$ compared to simple hydrogel. **C** Skin penetration of FENR after treatment with the binary ethosome dispersion and ethosomal hydrogel. As control, a FENR solution in isopropyl myristate was used. For the *stratum corneum*, the measured FENR concentrations were significantly lesser for the binary ethosomes and ethosomal hydrogel compared to control (**** $p < 0.001$). FENR content assessed in the epidermis + dermis without *stratum corneum* indicated that binary ethosomes resulted in significantly higher drug amounts than control (*** $p < 0.01$). Ethosome dispersion and ethosomal hydrogel enabled FENR delivery across the skin (in the RP)

the skin surface intact, leaving no residue on the tissue. Cleaning the skin upon removal of the ethosome dispersion and the control solution was more challenging because the formulations are liquid.

FENR delivery to the epidermis + dermis (ED) upon treatment with the ethosome dispersion was 2.6- and 3.5-fold higher compared to the ethosomal hydrogel and the control solution, respectively. The smaller amount of drug delivered by the ethosomal hydrogel might be attributed to the slower release of FENR compared to the ethosome dispersion. FENR was quantified in the receptor phase (RP) when both ethosomes and the hydrogel were used, indicating transdermal delivery. The results demonstrate that formation of the hydrogel did not preclude the vesicle ability to promote percutaneous delivery, enabling a more prolonged release without avoiding transdermal delivery. Previously, it had also been that demonstrated that the incorporation of deformable liposomes in vehicles like creams and gels did not alter the skin permeation of the molecules loaded in the vesicles (52).

Ethosomes have been demonstrated to disturb the lipid domain of the SC and might promote dissolution and extraction of intercellular lipids and alter their transition temperature, affecting the barrier function (53). It has also been suggested that ethosomes might penetrate the SC mainly through the intercellular route, with phospholipids being retained in the upper epidermis (53). Additionally, the combination of ethanol and lipid vesicles might potentiate SC fluidity enhancement and facilitate drug transport into deeper cutaneous layers and across the tissue (9, 53). Finally, transfollicular pathway could also contribute to penetration of vesicles into the deeper layers (52). All these mechanisms might participate at various levels on FENR skin penetration.

As proof of concept that binary ethosomes favor drug penetration, confocal microscopy was employed to visualize the cutaneous distribution of rhodamine B (as model compound) mediated by the binary ethosome dispersion. As can be observed in Fig. 6, the nanocarriers indeed improved the amount of rhodamine that penetrated at greater depths

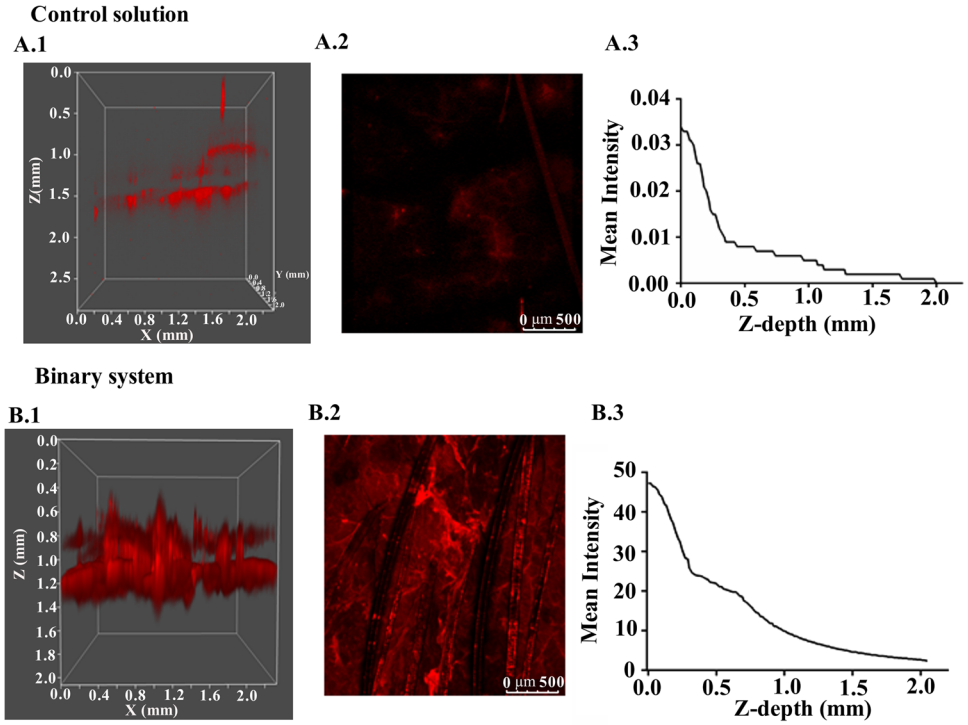

Fig. 6 Confocal laser scanning microscopy images depicting the depth of cutaneous penetration of the fluorescent dye rhodamine B (0.25% w/v) as hydrophobic drug model. Depth of rhodamine penetration from isopropyl myristate control solution (**A**.1) and binary ethosomes (**B**.1) in a 3D perspective of the skin and images of the tissue after treatment with isopropyl myristate (**A**.2) and binary ethosomes (**B**.2). The panel also shows fluorescence intensity as a function of depth (stacks) after treatment with isopropyl myristate (**A**.3) and in binary ethosomes (**B**.3)

of the skin compared to a solution. Moreover, it is possible to observe that fluorescence was homogenously distributed on the cutaneous surface, suggesting that penetration might occur through the intact stratum corneum and not only through skin appendages. Therefore, these results indicate the benefit of including binary ethosomes in pharmaceutically acceptable dosage forms for an improved penetration.

Formulation Cytotoxicity

Before assessing formulation cytotoxicity, it was important to investigate whether the hydrogel could be dispersed in the culture medium and whether it affected the ethosome size distribution. The hydrogel could be dispersed in supplemented DMEM-F12 medium with vortex mixing at the same concentration range selected for the cell cytotoxicity assay (sodium alginate at 1–100 µg/mL). The DLS data obtained using number distribution indicated the presence of a peak that corresponded to vesicles, suggesting that the cell culture medium did not destroy the vesicles (Figure S2).

Compared to the drug solution, the ethosomal hydrogel decreased the IC_{50} values of FENR in MCF-7 cells (Fig. 7A). The alginate dispersion, employed as a control, also reduced the MCF-7 cell viability when its concentration was 10 µg/mL (Fig. 7B). According to the ISO 10993–5:2009, viability reductions to values lower than 70% are considered a cytotoxic effect, and thus, this concentration can be cytotoxic. Images of untreated and treated cells (at IC_{50} values) are depicted in Figure S3.

The increase of FENR cytotoxic potential in MCF-7 cells mediated by its incorporation in the ethosomal hydrogel compared to the drug solution might be justified by two

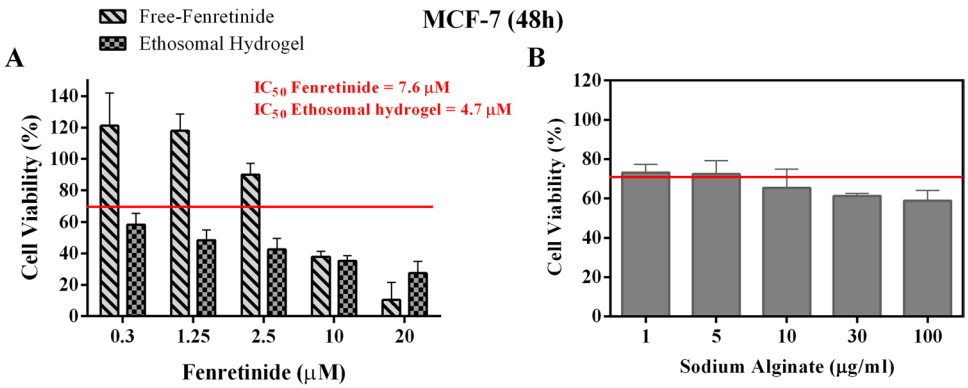

Fig. 7 *In Vitro* cell viability (%) for MCF-7 cells. **A** Viability after exposition to a fenretinide solution (free-fenretinide) and the fenretinide-loaded ethosomal hydrogel over 48 h. **B** *In Vitro* cytotoxicity of blank ethosomal hydrogel for MCF-7 cells line over 48 h. The red line indicates viability of 70%, which correspond to the initial cytotoxicity according to the ISO 10993–5:2009

facts. First, presence of ethanol in the formulations could lead to a higher concentration-dependent cytotoxicity (54). Second, sodium alginate could have influenced these effects since, according to Mishra *et al.* (2021), unloaded carriers of sodium alginate presented cytotoxicity for primary cells of mouse lymphocytes at a concentration of 10 µg/mL (55). Likewise, it has been reported that alginate nanoparticles enhanced the *in vitro* anticancer action of doxorubicin (56) and tamoxifen in MCF-7 cells (57).

CONCLUSIONS

The formation of hydrogel based on ethosomes and sodium alginate led to technological advantages as increased viscosity and bioadhesion compared to the conventional hydrogel without vesicles, suggesting that the lipid vesicles contribute to the gelling process. An enhanced performance of the ethosomal-based hydrogel was achieved compared to ethosomes for fenretinide release with initial burst release followed by a slow release, which is ideal for topical formulations. Although we observed a lower retention of fenretinide in skin layers, especially in the *stratum corneum*, the hydrogel did not preclude drug transdermal delivery, resulting in values similar to those provided by the ethosome dispersion. These results suggest that the ethosomal hydrogel provides a more prolonged drug penetration. Finally, fenretinide incorporation in the ethosomal hydrogel resulted in improved cytotoxicity against MCF-7 cells. The technological advantages of the ethosomal hydrogel can be further explored in suitable prolonged release formulations based on nanotechnology.

Supplementary Information The online version contains supplementary material available at https://doi.org/10.1208/s12249-022-02257-1.

Acknowledgements The authors would like to acknowledge Dr. Leticia Costa-Lotufo (Institute of Biomedical Sciences, University of Sao Paulo) for use of the cell culture facility.

Author Contribution Conceptualization—A.C.A. and L.B.L.; confocal microscopy assay—M.M.S.; HET-CAM and rheology assay—G.C.S.; bioadhesion: M.C.; writing—original draft preparation—A.C.A., M.C. and L.B.L.; funding acquisition—L.B.L.

Funding This study was supported by São Paulo Research Foundation (FAPESP, grant# 2018/ 13877–1) and CAPES (finance code 001). Fellowships from FAPESP (grant# 2018/14375–0 to A.C. Apolinário) and National Council of Technological and Scientific Development (306866/2020–0 to L.B. Lopes) are greatly appreciated. This study is part of the National Institute of Science and Technology in Pharmaceutical Nanotechnology: a transdisciplinary approach INCT-NANOFARMA, which is supported by FAPESP (grant #2014/50928–2) and CNPq (grant # 465687/2014–8). The authors are grateful to CENTD for support with the confocal microscopy facility. CENTD is supported by São Paulo Research Foundation (FAPESP) grant number 2020/13139–0 (FAPESP/GSK/Instituto Butantan).

Declarations

Conflict of Interest The authors filed for a patent application in Brazil in a topic related to this study.

References

1. Veronesi U, Mariani L, Decensi A, Formelli F, Camerini T, Miceli R, *et al*. Fifteen-year results of a randomized phase III trial of fenretinide to prevent second breast cancer. Ann Oncol. 2006;17:1065–71.
2. Cooper JP, Reynolds CP, Cho H, Kang MH. Clinical development of fenretinide as an antineoplastic drug: pharmacology perspectives. Exp Biol Med. 2017;242:1178–84.
3. Apolinário AC, Hauschke L, Nunes JR, Lopes LB. Towards nanoformulations for skin delivery of poorly soluble API: what does indeed matter? J Drug Deliv Sci Technol. 2020;60:1–13.
4. Mojeiko G, Passos JS, Apolinario AC, Lopes LB. Topical transdermal chemoprevention of breast cancer: where will nanomedical approaches deliver us? Nanomedicine. 2021;16:1713–31.
5. Narvekar M, Xue HY, Eoh JY, Wong HL. Nanocarrier for poorly water-soluble anticancer drugs—barriers of translation and solutions. AAPS PharmSciTech. 2014;15:822–33.
6. Lee O, Khan SA. Novel routes for administering chemoprevention: local transdermal therapy to the breasts. Semin Oncol. 2016;43:107–15. https://doi.org/10.1053/j.seminoncol.2015.09.003.
7. Lee O, Ivancic D, Allu S, Shidfar A, Kenney K, Helenowski I, *et al*. Local transdermal therapy to the breast for breast cancer prevention and DCIS therapy: preclinical and clinical evaluation. Cancer Chemother Pharmacol. 2015;76:1235–46.
8. Bulbake U, Doppalapudi S, Kommineni N, Khan W. Liposomal formulations in clinical use: an updated review development. Pharmaceutics. 2017;9:1–33.
9. Touti R, Noun M, Guimberteau F, Lecomte S, Faure C. What is the fate of multi-lamellar liposomes of controlled size, charge and elasticity in artificial and animal skin? Eur J Pharm Biopharm. 2020;151:18–31. https://doi.org/10.1016/j.ejpb.2020.03.017.
10. Apolinário AC, Hauschke L, Nunes JR, Lopes LB. Lipid nanovesicles for biomedical applications: 'What is in a name'? Prog Lipid Res. 2021;82:101096.
11. Apolinário AC, Hauschke L, Nunes JR, Lourenço Felipe Rebello, Lopes LB. Design of multifunctional ethosomes for topical fenretinide delivery and breast cancer chemoprevention. Colloids Surfaces A Physicochem Eng Asp. 2021;623:126745.
12. Rehman K, Zulfakar MH. Recent advances in gel technologies for topical and transdermal drug delivery. Drug Dev Ind Pharm. 2014;40:433–40.
13. ICCVAM. Test method evaluation report: current validation status of in vitro test methods proposed for identifying eye injury hazard potential of chemicals and products (volume 2) Interagency Coordinating Committee on the Validation of Alternative Methods Nationa. 2010;2. Available from: https://ntp.niehs.nih.gov/iccvam/docs/ocutox_docs/invitro-2010/tmer-vol2.pdf
14. Hosmer JM, Steiner AA, Lopes LB. Lamellar liquid crystalline phases for cutaneous delivery of paclitaxel: impact of the monoglyceride. Pharm Res. 2013;30:694–706.
15. Trivedi R, Umekar M, Kotagale N, Bonde S, Taksande J. Design, evaluation and in vivo pharmacokinetic study of a cationic flexible liposomes for enhanced transdermal delivery of pramipexole. J Drug Deliv Sci Technol. 2021;61: 102313. https://doi.org/10.1016/j.jddst.2020.102313.

16. Shah H, Nair AB, Shah J, Jacob S, Bharadia P, Haroun M. Proniosomal vesicles as an effective strategy to optimize naproxen transdermal delivery. J Drug Deliv Sci Technol. 2021;63:102479. https://doi.org/10.1016/j.jddst.2021.102479.
17. Marwah MK, Shokr H, Sanchez-Aranguren L, Badhan RKS, Wang K, Ahmad S. Transdermal delivery of a hydrogen sulphide donor, ADT-OH using aqueous gel formulations for the treatment of impaired vascular function: an ex vivo study. Pharm Res Pharmaceutical Research. 2022;39:341–52.
18. Kuznetsova DA, Vasileva LA, Gaynanova GA, Vasilieva EA, Lenina OA, Nizameev IR, *et al*. Cationic liposomes mediated transdermal delivery of meloxicam and ketoprofen: Optimization of the composition, in vitro and in vivo assessment of efficiency. Int J Pharm. 2021;605:120803. https://doi.org/10.1016/j.ijpharm.2021.120803.
19. Altamimi MA, Hussain A, Alrajhi M, Alshehri S, Imam SS, Qamar W. Luteolin-loaded elastic liposomes for transdermal delivery to control breast cancer: *in vitro* and ex vivo evaluations. Pharmaceuticals. 2021;14.
20. Altamimi MA, Hussain A, Alshehri S, Imam SS. Experimental design based optimization and ex vivo permeation of desmopressin acetate loaded elastic liposomes using rat skin. Pharmaceutics. 2021;13.
21. Ali AA, Hassan AH, Eissa EM, Aboud HM. Response surface optimization of ultra-elastic nanovesicles loaded with deflazacort tailored for transdermal delivery: accentuated bioavailability and anti-inflammatory efficacy. Int J Nanomedicine. 2021;16:591–607.
22. Jain A, Jain SK. *In vitro* release kinetics model fitting of liposomes: an insight. Chem Phys Lipids. 2016;201:28–40. https://doi.org/10.1016/j.chemphyslip.2016.10.005.
23. Haidar ZS, Hamdy RC, Tabrizian M. Protein release kinetics for core-shell hybrid nanoparticles based on the layer-by-layer assembly of alginate and chitosan on liposomes. Biomaterials. 2008;29:1207–15.
24. Fonseca-Santos B, Satake CY, Calixto GMF, Dos Santos AM, Chorilli M. Trans-resveratrol-loaded nonionic lamellar liquid-crystalline systems: structural, rheological, mechanical, textural, and bioadhesive characterization and evaluation of in vivo anti-inflammatory activity. Int J Nanomedicine. 2017;12:6883–93.
25. Carvalho V, Lemos DP, Vieira CS, Migotto A, Lopes LB. Potential of non-aqueous microemulsions to improve the delivery of lipophilic drugs to the skin. AAPS PharmSciTech AAPS PharmSciTech. 2017;18:1739–49.
26. Pepe D, Carvalho VFM, McCall M, De Lemos DP, Lopes LB. Transportan in nanocarriers improves skin localization and antitumor activity of paclitaxel. Int J Nanomedicine. 2016;11:2009–19.
27. Mosmann T. Rapid colorimetric assay for cellular growth and survival: application to proliferation and cytotoxicity assays. J Immunol Methods. 1983;65:55–63.
28. Salata GC, Malagó ID, Carvalho Dartora VFM, Marçal Pessoa AF, Fantini MC de A, Costa SKP, *et al*. Microemulsion for prolonged release of fenretinide in the mammary tissue and prevention of breast cancer development. Mol Pharm. American Chemical Society (ACS); 2021;
29. Shapiro YE. Structure and dynamics of hydrogels and organogels: an NMR spectroscopy approach. Prog Polym Sci. 2011;36:1184–253. https://doi.org/10.1016/j.progpolymsci.2011.04.002.
30. Ahmed EM. Hydrogel : Preparation, characterization, and applications: a review. J Adv Res Cairo University. 2015;6:105–21. https://doi.org/10.1016/j.jare.2013.07.006.
31. Lee KY, Mooney DJ. Alginate: properties and biomedical applications. Prog Polym Sci. 2012;37:106–26. https://doi.org/10.1016/j.progpolymsci.2011.06.003.
32. El Kechai N, Bochot A, Huang N, Nguyen Y, Ferrary E, Agnely F. Effect of liposomes on rheological and syringeability properties of hyaluronic acid hydrogels intended for local injection of drugs. Int J Pharm. 2015;487:187–96. https://doi.org/10.1016/j.ijpharm.2015.04.019.
33. Heatley F, Scott JE. A water molecule participates in the secondary structure of hyaluronan. Biochem J. 1988;254:489–93.
34. Ionov R, El-Abed A, Goldmann M, Peretti P. Interactions of lipid monolayers with the natural biopolymer hyaluronic acid. Biochim Biophys Acta - Biomembr. 2004;1667:200–7.
35. Duro-Castano A, Poma A, Pessoa A, Bueno CZ, Apolina AC, Rangel-yagui CO, et al. L - asparaginase encapsulation into asymmetric permeable polymersomes. Acs Macro Lett. 2020;9:1471–7.
36. Devi N, Kakati DK. Smart porous microparticles based on gelatin/sodium alginate polyelectrolyte complex. J Food Eng Elsevier Ltd. 2013;117:193–204. https://doi.org/10.1016/j.jfoodeng.2013.02.018.
37. Shen LN, Zhang YT, Wang Q, Xu L, Feng NP. Enhanced in vitro and in vivo skin deposition of apigenin delivered using ethosomes. Int J Pharm. 2014;460:280–8. https://doi.org/10.1016/j.ijpharm.2013.11.017.
38. Junqueira Garcia MT, Pedralino Gonçalves T, São Félix Martins É, Silva Martins T, de Abreu Carvalho, Fantini M, RegaziMinarini PR, et al. Improvement of cutaneous delivery of methylene blue by liquid crystals. Int J Pharm. 2018;548:454–65.
39. Mojeiko G, de Brito M, Salata GC, Lopes LB. Combination of microneedles and microemulsions to increase celecoxib topical delivery for potential application in chemoprevention of breast cancer. Int J Pharm Elsevier. 2019;560:365–76. https://doi.org/10.1016/j.ijpharm.2019.02.011.
40. U.S. Food and Drug Administration. Inactive ingredient search for approved drug products [Internet]. U.S. Food Drug Adm. 2020 [cited 2021 Mar 15]. Available from: https://www.accessdata.fda.gov/scripts/cder/iig/index.cfm
41. Camelo SRP, Franceschi S, Perez E, Fullana SG, Ré MI. Factors influencing the erosion rate and the drug release kinetics from organogels designed as matrices for oral controlled release of a hydrophobic drug. Drug Dev Ind Pharm. 2016;42:985–97.
42. Mircioiu C, Voicu V, Anuta V, Tudose A, Celia C, Paolino D, et al. Mathematical modeling of release kinetics from supramolecular drug delivery systems. Pharmaceutics. 2019;11:1–45.
43. Marcos LB. Mathematical models of drug release. In: Bruschi ML, editor. Strategies to modify drug release from pharmaceutical systems. Elsevier; 2015. p. 63–86.
44. Shetty S, Jose J, Kumar L, Charyulu RN. Novel ethosomal gel of clove oil for the treatment of cutaneous candidiasis. J Cosmet Dermatol. 2019;18:862–9.
45. Glavas-Dodov M, Fredro-Kumbaradzi E, Goracinova K, Simonoska M, Calis S, Trajkovic-Jolevska S, et al. The effects of lyophilization on the stability of liposomes containing 5-FU. Int J Pharm. 2005;291:79–86.
46. Fathalla D, Youssef EMK, Soliman GM. Liposomal and ethosomal gels for the topical delivery of anthralin: preparation, comparative evaluation and clinical assessment in psoriatic patients. Pharmaceutics. 2020;12:1–24.
47. Yoon HY, Kwak SS, Jang MH, Kang MH, Sung SW, Kim CH, et al. Docetaxel-loaded RIPL peptide (IPLVVPLRRRRRRRRC)-conjugated liposomes: drug release, cytotoxicity, and antitumor efficacy. Int J Pharm. 2017;523:229–37. https://doi.org/10.1016/j.ijpharm.2017.03.045.
48. Smart JD. The basics and underlying mechanisms of mucoadhesion. Adv Drug Deliv Rev. 2005;57:1556–68.
49. Woodley J. Bioadhesion new possibilities for drug administration? Clin Pharmacokinet. 2001;40:77–84.
50. Jin SG, Yousaf AM, Kim KS, Kim DW, Kim DS, Kim JK, et al. Influence of hydrophilic polymers on functional properties and wound healing efficacy of hydrocolloid based wound dressings. Int J Pharm. 2016;501:160–6. https://doi.org/10.1016/j.ijpharm.2016.01.044.

51. Frank LA, Chaves PS, D'Amore CM, Contri RV, Frank AG, Beck RCR, et al. The use of chitosan as cationic coating or gel vehicle for polymeric nanocapsules: increasing penetration and adhesion of imiquimod in vaginal tissue. Eur J Pharm Biopharm. 2017;114:202–12. https://doi.org/10.1016/j.ejpb.2017.01.021.
52. Izquierdo MC, Lillo CR, Bucci P, Gómez GE, Martínez L, Alonso V, et al. Comparative skin penetration profiles of formulations including ultradeformable liposomes as potential nanocosmeceutical carriers. J Cosmet Dermatol. 2020;19:3127–37.
53. Niu X, Zhang D, Bian Q, Feng X, Li H, Rao Y. Mechanism investigation of ethosomes transdermal permeation. Int J Pharm X. 2019;1:100027. https://doi.org/10.1016/j.ijpx.2019.100027.
54. Zhang Y, Ng W, Hu J, Saleh S, Ge Y, Xu H. Formulation and *in vitro* stability evaluation of ethosomal carbomer hydrogel for transdermal vaccine delivery. Colloids Surfaces B Biointerfaces. 2018;163:184–91. https://doi.org/10.1016/j.colsurfb.2017.12.031.
55. Mishra A, Pandey VK, Shankar BS, Melo JS. Spray drying as an efficient route for synthesis of silica nanoparticles-sodium alginate biohybrid drug carrier of doxorubicin. Colloids Surfaces B Biointerfaces. 2021;197: 111445. https://doi.org/10.1016/j.colsurfb.2020.111445.
56. Gong T. Improvement of *in vitro* anticancer activity of doxorubicin by sodium alginate nanoparticles delivery. J Pharm Biomed Sci. 2018;08:89–93.
57. Rossi T, Iannuccelli V, Coppi G, Bruni E, Baggio G. Role of the pharmaceutical excipients in the tamoxifen activity on MCF-7 and vero cell cultures. Anticancer Res. 2009;29:4529–33.